

1  
2  
3  
4 **Tribological behaviour of novel chemically modified biopolymer-thickened**  
5 **lubricating greases investigated in a steel-steel rotating ball-on-three plates**  
6  
7 **tribology cell**  
8  
9

10  
11  
12  
13  
14  
15 R. Gallego<sup>1</sup>, T. Cidade<sup>2</sup>, R. Sánchez<sup>1</sup>, C. Valencia<sup>1,3</sup>, J.M. Franco<sup>1,3</sup>, ✉  
16  
17

18 <sup>1</sup> Dept. Ingeniería Química, Química Física y Química Orgánica. Campus de “El Carmen”.  
19 Universidad de Huelva. 21071 Huelva. Spain. Campus de Excelencia Internacional  
20 Agroalimentario, ceiA3.  
21  
22

23 <sup>2</sup> Dept. Ciência dos Materiais and Cenimat/I3N, Universidad Nova de Lisboa, P-2829-516  
24 Caparica, Portugal.  
25  
26

27 <sup>3</sup> Pro<sup>2</sup>TecS – Chemical Process and Product Technology Research Center. Universidad de  
28 Huelva. 21071 Huelva. Spain.  
29  
30  
31  
32  
33  
34  
35  
36  
37  
38  
39  
40  
41  
42  
43  
44  
45  
46  
47  
48  
49

50 ✉ Author to whom correspondence should be addressed:  
51

52 Prof. J.M. Franco. Departamento de Ingeniería Química, Química Física y Química Orgánica.  
53 Campus de “El Carmen”. Universidad de Huelva. 21071 Huelva. Spain.  
54  
55

56 Phone: +34959219995, Fax: +34959219983, e-mail: [franco@uhu.es](mailto:franco@uhu.es)  
57  
58  
59  
60  
61  
62  
63  
64  
65

## Abstract

In this work, model renewable and biodegradable lubricating greases based on castor oil and chemically modified biopolymers (methylcellulose, chitin and cellulosic pulp) were tribologically characterized in a steel-steel ball-on-plates tribological cell coupled to a controlled-stress rheometer, and the results were compared to those provided by conventional lithium and calcium soap-based greases. Viscous flow, sliding velocity sweep and transient friction tests were carried out and resulting wear scars in the steel plates were evaluated by means of scanning electron microscopy (SEM). Different frictional responses were found depending on the thickener, especially at high temperature. Excepting for most severe conditions, wear is negligible when using chemically modified chitin and methylcellulose-based greases as lubricants.

**Keywords:** Biopolymer-based lubricating greases; friction; rheology; wear.

## INTRODUCTION

Lubricating greases are highly structured suspensions in which the core composition consists of a thickening agent dispersed in a lubricating base oil, optionally complemented with additives in order to improve some specific properties and functions [1]. Nowadays, commercial lubricating greases are mostly mineral oil-based whereas most commonly used thickeners are fatty acid soaps of lithium, calcium and aluminium, di- or polyureas and inorganic thickeners like clays and silica derivatives. Observations by electron and atomic force microscopy [2,3] revealed that the thickener forms a network, with different structure depending on the thickener agent, that traps the oil and confers the desired rheological properties [4,5]. These particular rheological characteristics imparted by the thickener make lubricating greases more convenient in some applications where lubricating oils do not work properly. Actually, factors like decreasing leakage and frequency of lubrication in hard-to-reach contacts, fluctuations with temperature, loads, vibrations, etc. can be minimized when using greases [6]. In addition, lubricating greases can absorb contaminants, such as particles and water, in relatively large amounts, without reduction in its lubricating properties thus acting as effective seals [7,8]. As previously reviewed [6], the mechanisms of grease lubrication in bearings are still under discussion. In the past [9,10], the lubricating function of greases was only attributed to the ability of the base oil to bleed in a lubricated contact, however, more recent works highlight the importance of thickener particles on contact surfaces [11-13]. The presence of the thickener particles give rise to an increase in the effective viscosity and thickness of the elastohydrodynamic lubrication film [14-17], resulting in a significant reduction of the friction coefficient with respect to those found for the base oil alone. Therefore the thickener also plays an important role in the lubrication process.

The preservation of the environment, as well as the corresponding governmental directives in numerous countries, promotes the increasing introduction of renewable raw materials in different industrial applications, namely in the lubricant industry [18]. As extensively reported [19-21], the use of vegetable oils is gaining some importance due to a number of valuable

1 characteristics such as high lubricity, easy adhesion to metal surfaces, weak viscosity-  
2 temperature dependence, low volatility, solvency for lubricant additives, easy miscibility with  
3 other fluids, low toxicity and high biodegradability. Despite limitations such as poor thermo-  
4 oxidative stability, deficient low temperature flow properties due to crystallization and small  
5 range of viscosities that restrict the applicability of vegetable oils, previous studies  
6 demonstrated that these disadvantages can be overcome using proper additives [22-26].  
7 However, global production of vegetable oil-based greases is marginal so far, i.e. lower than  
8 1%, as a consequence of still poorer performance characteristics [27]. The development of fully  
9 bio-based lubricating greases is even a more challenging issue that needs not only the  
10 replacement of the mineral oil by a suitable vegetable one but also the selection of an  
11 appropriate thickening agent obtained from renewable resources. Oil substitution has been  
12 satisfactorily addressed [28-30], but the replacement of the thickener is a much more complex  
13 task to solve due to the high technical efficiency of traditional metallic soaps and urea  
14 derivatives, which impart the desired rheological, thermal and tribological properties to the bulk  
15 system. Up to now, vegetable oil-based calcium soap- or clay-thickened greases are considered  
16 environmentally-friendly, although showing some performance limitations like, for instance, the  
17 lower thermal resistance of calcium greases. Some lubricating greases based on biodegradable  
18 oils with traditional thickeners were tested in different tribological contacts [28,31] showing low  
19 values of friction coefficient and small wear scar size for some specific formulations, basically  
20 depending on the balance between oil polarity and type of thickener.  
21  
22  
23  
24  
25  
26  
27  
28  
29  
30  
31  
32  
33  
34  
35  
36  
37  
38  
39  
40  
41  
42  
43  
44

45 Previous research reported the formulation of oleogels thickened with cellulose derivatives  
46 which exhibit satisfactory mechanical and physical stabilities as well as more accurate thermal  
47 resistance than that found for conventional lubricating greases [32-34]. However, in these cases,  
48 suitable mechanical and physical stabilities were linked to much higher values of the linear  
49 viscoelastic functions than those found for standard greases. More promising results were  
50 recently found when using diisocyanate compounds to either functionalize biopolymers with  
51 reactive groups [35,36] or create an extensively crosslinked network [37] able, in both cases, to  
52  
53  
54  
55  
56  
57  
58  
59  
60  
61  
62  
63  
64  
65

1 retain the base oil. Despite the fact that isocyanate compounds may be considered hazardous,  
2 when the biopolymer is dispersed in castor oil, there is no more free NCO groups but urethane  
3 linkages, formed after the chemical reaction between NCO and hydroxyl groups located in the  
4 ricinoleic fatty acid chain. Therefore, the thickener chemically interacts with the base oil,  
5 resulting in the oleogel physical stabilization [38]. As has been reported, polyurethanes based on  
6 biodegradable polyols [39], and particularly biopolymers containing urethane and carbamate  
7 linkages [40], are considered largely biodegradable materials. Taking into account all the  
8 previous research on the finding of proper new bio-based thickeners and, especially, considering  
9 the suitable rheological behaviour of formulations based on biopolymers chemically modified  
10 with isocyanate compounds, the objective of this work was to offer new experimental  
11 tribological data of NCO-modified methylcellulose, chitin and cellulosic pulp dispersions in  
12 castor oil. These formulations, completely based on renewable resources have been selected as  
13 promising grease candidates. Their performance has been compared with those found in two  
14 commercial formulations based on lithium and calcium soaps.

## 33 **EXPERIMENTAL**

### 36 **Materials**

39 Castor oil purchased from Guinama (Spain) was selected as vegetable oil medium to prepare  
40 oleogel formulations. Viscosity values of castor oil are 550 and 8.25 cP at 25 and 125 °C,  
41 respectively [41]. Methylcellulose ( $M_n$ : 40000 g·mol<sup>-1</sup>; DS: 1.6-1.9), acquired from Sigma-  
42 Aldrich; chitin ( $M_n$ : 5.4×10<sup>5</sup> g·mol<sup>-1</sup>; degree of deacetylation: 7.3%), purchased from Qingdao  
43 Fraken (China), and commercial grade Kraft cellulose pulp from *Eucalyptus globulus*, kindly  
44 supplied by ENCE, S.A. (Huelva factory, Spain), were used as thickening agents after  
45 modification with 1,6-hexamethylene diisocyanate (HMDI, purum grade, ≥98.0%). HMDI and  
46 all other common reagents and solvents employed were supplied by Sigma-Aldrich. Details of  
47 biopolymer chemical modifications with HMDI can be found elsewhere [35-38]. Two  
48 commercial lubricating greases were used as benchmarks: a conventional mineral oil-based  
49

1  
2 lithium grease (Castrol, Germany) and one considered biodegradable based on castor oil and an  
3 anhydrous calcium thickener (kindly supplied by Verkol, Spain).  
4

### 5 **Manufacture of model biopolymer-based lubricating greases**

6

7  
8 The dispersion of the thickeners in the base oil was carried out in an open vessel, using a  
9 controlled-rotational speed mixing device (70 rpm) RW 20 (Ika), equipped with an anchor  
10 impeller. NCO-functionalized methylcellulose and chitin were slowly added to the castor oil at  
11 the same concentration (30% (w/w)), whereas the thickener based on cellulosic pulp was used in  
12 a concentration of 7% w/w. The mixing process was maintained at 70 rpm for 24 hours at room  
13 temperature. Finally, the resulting dispersion was homogenized with an Ultra-Turrax T50 (Ika)  
14 rotor-stator turbine, at 8800 rpm for 1 min in the case of the methylcellulose and chitin-based  
15 oleogels and 5 min for the cellulosic pulp-based oleogel, and afterwards they were de-aerated by  
16 applying vacuum. Table 1 summarises the composition of the different formulations obtained  
17 along with identifying codes and basic technical data. Commercial grease samples and  
18 composition of biopolymer-based greases were selected attending to their similar rheological  
19 response previously analysed [35-37].  
20  
21  
22  
23  
24  
25  
26  
27  
28  
29  
30  
31  
32  
33  
34  
35

### 36 **Atomic force microscopy (AFM)**

37

38  
39 Microstructures of the two commercial greases (LI and CA samples) were obtained by means of  
40 atomic force microscopy (AFM) with a Multimode apparatus connected to a Nanoscope-IV  
41 scanning probe microscope controller (Digital Instruments, Veeco Metrology Group Inc.).  
42 Images were acquired in the tapping mode using Veeco Nanoprobe™ tips. Samples were not  
43 submitted to any physical modification or partial oil extraction but previously heated below the  
44 dropping point. Therefore, this technique allows obtaining the microstructure of untreated  
45 samples. LI and CA microstructures are shown in Figure 1 and may be compared to those  
46 previously reported for the biopolymer-based greases studied [37,42], which display fibrous  
47 structures, more similar to the lithium grease.  
48  
49  
50  
51  
52  
53  
54  
55  
56  
57  
58  
59

### 60 **Rheological characterization**

61  
62  
63  
64  
65

1 Rheological characterization was carried out with a controlled-stress rheometer, Physica MCR-  
2 501 (Anton Paar, Austria). Viscous flow tests were performed applying a stepped shear rate  
3 ramp in a shear rate range of  $3 \cdot 10^{-3}$  to  $10^2 \text{ s}^{-1}$  at 25 and 125 °C. Rheological measurements were  
4 carried out using a plate–plate geometry (25 mm diameter, 1 mm gap) with grooved surfaces to  
5 overcome wall slip phenomena usually observed in lubricating greases [43]. At least two repeats  
6 of each test were performed on fresh samples.  
7  
8  
9  
10  
11  
12

### 13 **Tribological Tests**

14 Tribological tests were performed in a tribology measuring cell coupled to the Physica MCR-  
15 501 controlled-stress rheometers [44]. The cell uses a 6.35 mm diameter steel ball (1.4401 grade  
16 100) rotating on three 45° inclined steel plates (1.4301). The evolution of the friction  
17 coefficient,  $\mu$ , with the rotational speed was tested in a range of rotational velocities of 0.01-  
18 1000 rpm, at 25 and 125 °C and different normal loads (10, 20 and 40 N). These normal forces  
19 as well as sliding velocities were calculated from the applied axial force, ball radius and angular  
20 velocity according to Heyer and Lauger [44]. Estimated contact Hertzian pressures for each  
21 normal load applied are 1.29, 1.63 and 2.05 GPa, respectively. The stationary friction  
22 coefficient was also obtained at 25 and 125 °C by applying normal forces of 10, 20 and 40 N  
23 and setting a constant rotational speed (0.15, 10 and 400 rpm) for 10 min. Five repeats of each  
24 test were performed on fresh samples. Resulting wear scars on the steel plates were examined  
25 by triplicate using a scanning electronic microscope, model JSM-5410 (JEOL).  
26  
27  
28  
29  
30  
31  
32  
33  
34  
35  
36  
37  
38  
39  
40  
41  
42  
43  
44

## 45 **RESULTS AND DISCUSSION**

### 46 **Viscous flow behaviour**

47 Viscous flow curves of the lubricating greases studied were obtained at 25 and 125 °C. Figure 2  
48 shows the comparison at 25 °C, which reveals very similar viscosity values, excepting for  
49 sample CH which is more viscous in all the shear rate range studied. Shear rate range is limited  
50 due to the appearance of fracture at high or moderate shear rates [43-45], which is favoured with  
51  
52  
53  
54  
55  
56  
57  
58  
59  
60  
61  
62  
63  
64  
65

1 grooved measuring surfaces [46]. Resulting flow curves can be satisfactorily described by the  
2 well-known power-law model:  
3

$$4 \quad \eta = K \cdot \dot{\gamma}^{n-1} \quad (1)$$

5  
6  
7  
8 where  $K$  and  $n$  are the consistency and flow indexes, respectively. Fitting parameters are listed  
9 in Table 2 for the different samples and temperatures studied. As expected, the consistency  
10 index ( $K$ ) presents lower values at 125 °C with respect to those found at 25 °C. As previously  
11 mentioned, the highest consistency index at 25 °C was achieved by the oleogel based on  
12 chemically modified chitin (CH), and then followed by MC and CP, respectively. Commercial  
13 lubricating greases, LI and CA, present consistency indexes that are slightly lower than those  
14 obtained for the biopolymer-based formulations. On the other hand, consistency indexes of  
15 these model formulations showed intermediate values with respect to the commercial greases at  
16 125 °C, excepting for the sample CP, which exhibits lower value than CA. On the other hand,  
17 extremely low values of the flow index were generally obtained for all samples, which is  
18 characteristic of the typical yielding behaviour shown by these materials.  
19  
20  
21  
22  
23  
24  
25  
26  
27  
28  
29  
30  
31  
32

### 33 **Evolution of the friction coefficient with the sliding velocity**

34  
35  
36 The frictional behaviour of greases analysed as lubricants in the steel-steel ball-on-plates contact  
37 was first characterized by applying a rotational speed sweep. Figure 3 shows the friction  
38 coefficient vs. sliding velocity curves, at 25 and 125 °C, for the formulations studied and  
39 selected normal force (20 N). As can be observed, at 25 °C, the general progression from  
40 boundary to elastohydrodynamic lubrication regimes were found for all samples, excepting for  
41 CH which mainly displays the transition from the mixed lubrication to the elastohydrodynamic  
42 regimes (Figure 3i). However, when temperature was increased up to 125 °C, higher rotational  
43 speed values are generally needed to detect the increasing part of the frictional curve, i.e. the  
44 transition from the mixed to the elastohydrodynamic regimes. In fact, the final increasing part of  
45 the friction coefficient vs. the sliding velocity curve was not observed at 125 °C when applying  
46 the commercial lubricating greases used as benchmarks (Fig. 3b and 3d). On the contrary, the  
47  
48  
49  
50  
51  
52  
53  
54  
55  
56  
57  
58  
59  
60  
61  
62  
63  
64  
65



1 different lubrication regimes are still apparent at 125 °C for the model biopolymer-based greases  
2 studied.

3  
4  
5 The classical Stribeck curve relates the friction coefficient ( $\mu$ ) with the dimensionless Hersey  
6 number, which is used to describe the combined influence of dynamic viscosity ( $\eta$ ), rotational  
7 speed ( $\Omega$ ) and the normal contact load applied ( $F_N$ ) in journal bearings. Instead, in similar  
8 geometries and conditions to that used in this work, the so-called hydrodynamic Stribeck  
9 parameter is defined as [47,48]:  
10  
11  
12  
13  
14  
15

$$16 \quad S = \frac{\eta u_s}{F_N} \quad (2)$$

17  
18  
19  
20  
21  
22  
23 being  $u_s$ , the sliding velocity. This parameter takes into account the fluid film formation  
24 between the two surfaces in a tribo-contact and discriminates the lubrication regimes as  
25 boundary, mixed lubrication or (elasto)hydrodynamic [49]. The Stribeck curve is widely used to  
26 describe the lubrication regimes of Newtonian lubricating oils, including bio-based oils [47, 50-  
27 53]. However, this approach is not widely reported for lubricating greases as a consequence of  
28 the non-Newtonian character and the unknown properties of the active lubricant inside the  
29 contact [16]. Lu and Khonsari [54] and Gonçalves et al [55] proposed the inclusion of the  
30 viscosity of the base oil, assuming that under highly stressed conditions, like those achieved in a  
31 tribological contact, the microstructure of the grease is almost destroyed and the main  
32 responsible for lubrication is the base oil:  
33  
34  
35  
36  
37  
38  
39  
40  
41  
42  
43  
44

$$45 \quad S = \frac{\eta_{BO} u_s}{F_N} \quad (3)$$

46  
47  
48  
49  
50  
51 As Gonçalves et al pointed out [55], the bleed oil viscosity is not affected by the type and  
52 concentration of the thickener and, according to Palacios and Palacios [56], grease viscosity  
53 tends to reach the base oil viscosity at extremely high shear rates. Obviously, this rule cannot be  
54 directly followed when using polymeric additives able to modify the base oil viscosity [57].  
55  
56  
57  
58  
59  
60  
61  
62  
63  
64  
65

1  
2  
3  
4  
5  
6  
7  
8  
9  
10  
11  
12  
13  
14  
15  
16  
17  
18  
19  
20  
21  
22  
23  
24  
25  
26  
27  
28  
29  
30  
31  
32  
33  
34  
35  
36  
37  
38  
39  
40  
41  
42  
43  
44  
45  
46  
47  
48  
49  
50  
51  
52  
53  
54  
55  
56  
57  
58  
59  
60  
61  
62  
63  
64  
65

Moreover, the role of the thickener in the tribo-contact is not considered in eq. (3). Accepting the inclusion of the base oil viscosity in the Stribeck parameter, among all the lubricating grease samples studied only CA and MC display a simple tribological behaviour which acceptably leads to a unique Stribeck master curve by superimposing the frictional curves obtained at different temperatures and normal loads (Figures 4a and 4b). This means that base oil viscosity and normal load govern film formation in these two greases, as expected for a Newtonian lubricant. In the remaining formulations, a single Stribeck curve cannot be obtained. In particular, when using CP sample as lubricant, the shape of the friction coefficient vs. sliding speed curve did not significantly change by modifying normal force or temperature, displaying maximum and minimum values of the friction coefficient at approximately the same values of the sliding velocity. An intermediate behaviour was observed in the case of CH sample. Stribeck curves calculated at different normal load and temperature conditions overlap each other only in the elastohydrodynamic region, whereas a scatter in the friction coefficient values, generally decreasing with the applied normal force, was found in the mixed lubrication regime (Figure 4c). Therefore, in these cases, the role of the thickener in the film formation seems to be more evident and greatly influences the frictional behaviour.

### **Evolution of friction coefficient with time**

The evolution of friction coefficient with time at different normal loads and rotational speeds was analyzed for each sample. A comparison of transient values of the friction coefficient is shown in Figure 5 for the lubricating greases studied and selected conditions. Generally, at the beginning, the friction coefficient rapidly drops and then progressively decreases down to a stationary value. This evolution has been traditionally attributed to the formation of the protective lubricating film due to the rubbing action [58] and, particularly in greases, to the rheological resistance that the ball has to overcome to plough its way at the beginning of motion [28]. However, under certain conditions, i.e. high normal loads, some of the lubricating greases evaluated produce a slight increase of the friction coefficient after the first drop, probably as a consequence of the effect of resulting wear debris. At 25 °C, the lower values of the friction

1 coefficient were obtained by using sample MC as lubricant and conversely the higher friction  
2 was found with sample CP (Figure 5a). At this temperature, the effect of normal load is always  
3 that shown in Figure 5b for a selected sample. However, temperature greatly affects this  
4 tendency, as discussed below.  
5  
6

7  
8  
9 In general, a stationary value of the friction coefficient was achieved after approximately 5-6  
10 minutes when using the biopolymer-based greases as lubricants, whereas commercial samples  
11 needed longer times (8-10 min). The bar diagram shown in Figure 6 portrays the steady-state  
12 friction coefficient values obtained by applying normal loads of 10, 20 and 40 N at constant  
13 angular velocity of 10 rpm and temperatures of 25 and 125 °C, for each grease used as lubricant  
14 in the tribo-contact. Samples such as LI and CH display the same tendency at 25 and 125 °C,  
15 i.e. the friction coefficient decreases with the normal load. This is not the expected normal force  
16 influence in the boundary and mixed lubrication regimes [54] but it is consistent with the higher  
17 rheological resistance offered by the grease to the rotational motion at lower normal loads [28].  
18 Moreover, for both samples, the friction coefficient values are even lower at higher temperature,  
19 in accordance with the lower rheological resistance offered as a result of the thermally-induced  
20 softening of greases. At the same time, microstructure is better preserved at 125 °C in these two  
21 samples, showing the higher values of the consistency index (Table 2). As a consequence, it is  
22 presumed that at high temperature the rheological resistance to the motion is reduced but the  
23 entrainment of the whole lubricant into the contact takes place. On the other hand, greases CA,  
24 CP and MC follow the former trend at 25 °C, but completely the opposite at 125 °C. This effect  
25 may be attributed to the fact that these microstructures are more strongly affected by shear and  
26 temperature, as the lower values of the consistency index suggest (Table 2), resulting in a  
27 significant reduction of the effective viscosity and, therefore, in the lubricant film thickness,  
28 which favours wear, especially at higher normal loads, as discussed in the next section. In fact,  
29 this temperature is rather close to the dropping point in sample CA (see Table 1) and therefore a  
30 more significant softening and oil bleeding is expected. This hypothesis is supported by the fact  
31 that a single Stribeck master curve was obtained for CA and MC samples when using the base  
32  
33  
34  
35  
36  
37  
38  
39  
40  
41  
42  
43  
44  
45  
46  
47  
48  
49  
50  
51  
52  
53  
54  
55  
56  
57  
58  
59  
60  
61  
62  
63  
64  
65

oil viscosity to estimate the Stribeck parameter. Alternatively, MC and, in lower extent, CP microstructures may release much more oil at high temperature and normal loads, as observed after performing the frictional tests, thus locally producing, in some parts of the tribo-contact, an increase in the effective concentration of the cellulosic thickening agent, which can interact with the metallic contact surfaces, causing higher friction and wear.

Figure 7 shows the values of the stationary friction coefficient by applying 20 N normal force and rotational speeds of 0.15, 10 and 400 rpm, at both 25 and 125 °C. The friction coefficient obtained when using the commercial lubricating greases, LI and CA, and formulation CP as lubricants, at 25 °C, decreases with the rotational speed, whereas the opposite tendency is observed in the case of CH at 25 °C. The sample MC at 25 °C displays a particular behaviour that first exhibits a reduction of the friction coefficient from 0.15 to 10 rpm, but a notably higher value at 400 rpm. At 125 °C, the tendency followed by almost all the samples, excepting for CP, reveals an increase in the friction coefficient from 0.15 to 10 rpm and a diminution from 10 to 400 rpm. In the case of the formulation based on the cellulosic pulp, at 125 °C, a remarkably high value at 0.15 rpm can be observed; however, from 10 to 400 rpm, the friction coefficient raises with the rotational speed. These tendencies followed by the stationary friction coefficient in every case are absolutely consistent with the dynamic frictional measurements previously discussed, i.e. the sliding velocity curves, and reflect the different lubrication regimes.

## **Wear**

Wear scars generated in the plates of the tribological cell and the corresponding average diameter are shown in Table 3 for selected lubricating grease samples and conditions. As can be concluded from the images, wear mechanism is predominantly abrasive. As expected, the stronger normal load is applied, the wider wear scar is, as can be seen in the bar diagram in Figure 8, which summarizes the evolution of the scar size with the normal load, at 25 and 125 °C. However, temperature and normal load do not exert a significant influence when using the lithium grease as lubricant. Sample CP provide values of the average wear scar diameter

1 comparable to those found with the commercial greases, excepting for the highest normal load  
2 applied, and generally lower at high temperature (Figure 8). In the particular cases of MC and  
3  
4 CH, no wear evidence in the plates was observed, excepting for 20 and 40 N at 125 °C, being  
5  
6 especially wide for MC.  
7

8  
9 Figure 9 displays the average wear mark diameters obtained from the steel plates of the  
10 tribological cell after performing tests at 0.15, 10 and 400 rpm under 20 N at 25 and 125 °C,  
11  
12 respectively. As can be observed, the increase in wear diameter with the rotational velocity is  
13  
14 the predominant tendency, at both temperatures. Once again, the samples based on  
15  
16 methylcellulose (MC) and chitin (CH) only provide appreciable wear scars under specific  
17  
18 conditions. At 25 °C, steel plates only evidence wear scars at 400 rpm when using MC sample  
19  
20 as lubricant, whereas rather large scar diameters can be observed at 125 °C under 10 and 400  
21  
22 rpm conditions. In the case of CH, significant wear evidence can be only detected at 400 rpm  
23  
24 and 125 °C.  
25  
26  
27  
28  
29

## 30 **CONCLUSIONS**

31  
32  
33 Several new biodegradable model lubricating greases based on NCO-chemically modified  
34  
35 biopolymeric thickener agents were tribologically characterized. Results were compared with  
36  
37 those obtained when using conventional lithium and calcium soap-based greases with alike  
38  
39 rheological properties as lubricants. Viscous flow curves of all samples were very similar and  
40  
41 can be satisfactorily described by the traditional power-law model. Greases containing NCO-  
42  
43 functionalized chitin and methylcellulose exhibit higher consistency indexes at 25 °C, whereas  
44  
45 this parameter is higher for lithium soap and chitin-based greases at 125 °C, which is indicative  
46  
47 of microstructures with higher thermal resistance. In all cases, fracture phenomenon clearly  
48  
49 arises at moderate shear rates, which limits the study to not very high shear conditions.  
50  
51  
52  
53

54  
55 The general progression from boundary to elastohydrodynamic lubrication regimes were found  
56  
57 when using the biopolymer-based greases as lubricants in the steel-steel ball-on plates tribo-  
58  
59 contact, at both 25 and 125 °C, when performing sliding velocity sweep tests. However, the  
60  
61  
62  
63  
64  
65

1 elastohydrodynamic regime was not detected at 125 °C when using conventional greases. Only  
2 calcium soap and methylcellulose-based samples display a simple tribological behaviour which  
3  
4 leads to a unique Stribeck master curve by superimposing the frictional curves obtained at  
5  
6 different temperatures and normal loads, using the base oil viscosity in the hydrodynamic  
7  
8 Stribeck parameter. This fact suggests that the base oil governs film formation in these two  
9  
10 greases, whereas the thickener seems to play a key role in the remaining samples. The stationary  
11  
12 friction coefficient always decreases with the normal load applied at 25 °C. However, the  
13  
14 opposite tendency was found at 125 °C for calcium soap-, methylcellulose or, in lower extent,  
15  
16 cellulosic pulp-based greases as lubricants. These results depend on the balance between the  
17  
18 rheological resistance offered by the grease and the shear and temperature dependence of grease  
19  
20 microstructure. In this sense, particularly calcium soap and methylcellulose microstructures, are  
21  
22 more strongly affected by temperature giving rise to a significant reduction of the lubricant film  
23  
24 thickness which favours wear at 125 °C. This fact is especially evident at high normal loads.  
25  
26 However, excepting for such severe conditions, wear is negligible when using chemically  
27  
28 modified chitin and methylcellulose-based greases as lubricants, whereas cellulosic pulp-based  
29  
30 grease provides wear scars comparable to those found with the conventional lithium and  
31  
32 calcium greases.  
33  
34  
35  
36

### 37 38 **ACKNOWLEDGEMENTS**

39  
40  
41 This work is part of two research projects (CTQ2014-56038-C3-1R and TEP-1499) sponsored  
42  
43 by MINECO-FEDER and Junta de Andalucía programmes, respectively. One of the authors  
44  
45 (Rocío Gallego) has received a Ph.D. Research Grant (BES-2011-045029) from DIGICYT  
46  
47 (MINECO). The authors gratefully acknowledge the financial support. Maria Teresa Cidade  
48  
49 acknowledges the support of the Portuguese Foundation for Science and Technology through  
50  
51 Project PEst-C/CTM/LA0025/2013 and The Portuguese Society of Rheology (SPR) for her stay  
52  
53 in University of Huelva.  
54  
55  
56

### 57 58 **REFERENCES**

- 1  
2  
3 [1] NLGI. Lubricating Greases Guide. Kansas: National Lubricating Grease Institute; 1994.  
4  
5 [2] Sánchez MC, Franco JM, Valencia C, Gallegos C, Urquiola F, Urchegui R. Atomic force  
6  
7 microscopy and thermo-rheological characterisation of lubricating greases. Tribol Lett 2011; 41:  
8  
9 463–470.  
10  
11 [3] Shuff PJ, Clarke LJ. Imaging of lubricating oil insolubles by electron microscopy. Tribol Int  
12  
13 1991; 24: 381–387.  
14  
15 [4] Mas R, Magnin A. Rheology of colloidal suspensions: case of lubricating greases. J Rheol  
16  
17 1994; 38: 889–908.  
18  
19 [5] Delgado MA, Valencia C, Sánchez MC, Franco JM, Gallegos C. Influence of soap  
20  
21 concentration and oil viscosity on the rheology and microstructure of lubricating greases. Ind  
22  
23 Eng Chem Res 2006; 45: 1902–1910.  
24  
25  
26 [6] Lugt PM. A review on grease lubrication in rolling bearings. Tribol Trnas 2009; 52: 470–  
27  
28 480.  
29  
30  
31 [7] Hamnelid L. Introduction to rheology of lubricating greases. In: Balan C, editor. Rheology  
32  
33 of lubricating greases, Amsterdam: ELGI; 2000, p. 1–20.  
34  
35  
36 [8] Baart P, Lugt PM, Prakash, B. contaminant migration in the vicinity of a grease lubricated  
37  
38 bearing seal contact. J. Tribol. 2011; 133: article 041801.  
39  
40  
41 [9] Booser ER, Wilcock DF. Minimum oil requirements of ball bearings. Lubric. Eng. 1953; 9:  
42  
43 140-143.  
44  
45  
46 [10] Baker AE. Grease bleeding. A factor in ball bearing performance. NLGI Spokesman 1958;  
47  
48 22: 271-279.  
49  
50  
51 [11] Amstrom H, Venner CH. Soap thickener induced local pressure fluctuations in a grease  
52  
53 lubricated EHD point contact. J Eng Tribol 1994; 208: 191–198.  
54  
55  
56  
57  
58  
59  
60  
61  
62  
63  
64  
65

- 1  
2  
3  
4  
5  
6  
7  
8  
9  
10  
11  
12  
13  
14  
15  
16  
17  
18  
19  
20  
21  
22  
23  
24  
25  
26  
27  
28  
29  
30  
31  
32  
33  
34  
35  
36  
37  
38  
39  
40  
41  
42  
43  
44  
45  
46  
47  
48  
49  
50  
51  
52  
53  
54  
55  
56  
57  
58  
59  
60  
61  
62  
63  
64  
65
- [12] Hurley S. Infrared spectroscopic characterisation of grease lubricant films on metal surfaces. *NLGI Spokesman* 2000; 64: 13–21.
- [13] Cann PM, Hurley S. Friction properties of grease in elastohydrodynamic lubrication. *NLGI Spokesman* 2002; 66: 6–15.
- [14] Palacios JM, Cameron A, Arizmendi L. Film thickness of grease in rolling contacts. *ASLE Trans* 1981; 24: 474–478.
- [15] Hurley S, Cann PM. The influence of grease composition on film thickness in rolling contacts. *NLGI Spokesman* 1999; 63: 12–22.
- [16] Gonçalves D, Graça B, Campos AV, Seabra J, Leckner J, Westbroek R. On the film thickness behaviour of polymer greases at low and high speeds. *Tribol Int* 2015; 90: 435–444.
- [17] Cen H, Lugt, PM, Morales-Espejel G. On the film thickness of grease-lubricated contacts at low speeds. *Tribol. Trans.* 2014; 57: 668-678.
- [18] Hinman ML. Environmental characteristics of fuel and lubricants. In: Totten GE, Westbrook SR, Shah RJ, editors. *Fuels and Lubricants Handbook: Technology, Properties, Performance and Testing*, West Conshohocken: ASTM International; 2003, p. 885–909.
- [19] Salimon J, Salih N, Yousuf E. Biolubricants: raw materials, chemical modifications and environmental benefits. *Eur J Lipid Sci Technol* 2010; 112: 519–530.
- [20] Garcés R, Martínez-Force E, Salas JJ. Vegetable oil basestocks for lubricants. *Grasas Aceites* 2011; 62: 21–28.
- [21] Erhan SZ, Asadaukas S. 2000. Lubricants base stocks from vegetable oils. *Ind Crops Prod* 2000; 11: 277–282.
- [22] Erhan SZ, Sharma BK, Perez JM. Oxidation and low temperature stability of vegetable oil-based lubricants. *Ind Crops Prod* 2006; 24: 292–299.



- 1  
2 [23] Asadauskas S, Perez JM, Duda JL. Oxidative stability and antiwear properties of high oleic  
3 vegetable oils. *Lubr Eng* 1996; 52: 877–882.  
4
- 5 [24] Quinchia LA, Delgado MA, Valencia C, Franco JM, Gallegos C. Viscosity modification of  
6 high-oleic sunflower oil with polymeric additives for the design of new biolubricant  
7 formulations. *Environ Sci Tech* 2009; 43: 2060–2065.  
8  
9
- 10 [25] Quinchia LA, Delgado MA, Franco JM, Spikes HA, Gallegos C. Low-temperature flow  
11 behaviour of vegetable oil-based lubricants. *Ind Crops Prod* 2012; 37: 383–388.  
12  
13
- 14 [26] Karmakar G, Ghosh P. Green additives for lubricating oil. *ACS Sustain Chem Eng* 2013; 1:  
15 1364–1370.  
16  
17
- 18 [27] Honary L. Performance characteristics of soybean based greases thickened with clay,  
19 aluminum complex and lithium. *NLGI Spokesman* 2001; 65: 18-27.  
20  
21
- 22 [28] Fiedler M, Sánchez R, Kuhn E, Franco JM. Influence of oil polarity and material  
23 combination on the tribological response of greases formulated with biodegradable oils and  
24 bentonite and highly dispersed silica acid. *Lubr Sci* 2013; 25: 397–412.  
25  
26
- 27 [29] Dresel WH. Biologically degradable lubricating greases based on industrial crops. *Ind*  
28 *Crops Prod* 1994; 2: 281–288.  
29  
30
- 31 [30] Adhvaryu A, Sung C, Erhan SZ. Fatty acids and antioxidant effects on grease  
32 microstructures. *Ind Crops Prod* 2005; 21: 285–291.  
33  
34
- 35 [31] Fiedler M, Kuhn E, Franco JM, Litters T. Tribological properties of greases based on  
36 biogenic base oils and traditional thickeners in sapphire-steel contact. *Tribol Lett* 2011; 44:  
37 293–304.  
38  
39
- 40 [32] Sánchez R, Franco JM, Delgado MA, Valencia C, Gallegos C. Development of new green  
41 lubricating grease formulations based on cellulosic derivatives and castor oil. *Green Chem*  
42 2009; 11: 686–693.  
43  
44  
45  
46  
47  
48  
49  
50  
51  
52  
53  
54  
55  
56  
57  
58  
59  
60  
61  
62  
63  
64  
65

- 1  
2  
3  
4  
5  
6  
7  
8  
9  
10  
11  
12  
13  
14  
15  
16  
17  
18  
19  
20  
21  
22  
23  
24  
25  
26  
27  
28  
29  
30  
31  
32  
33  
34  
35  
36  
37  
38  
39  
40  
41  
42  
43  
44  
45  
46  
47  
48  
49  
50  
51  
52  
53  
54  
55  
56  
57  
58  
59  
60  
61  
62  
63  
64  
65
- [33] Sánchez R, Franco JM, Delgado MA, Valencia C, Gallegos C. Rheological and mechanical properties of oleogels based on castor oil and cellulosic derivatives potentially applicable as bio-lubricating greases: Influence of cellulosic derivatives concentration ratio. *J Ind Eng Chem* 2011; 17: 705–711.
- [34] Sánchez R, Franco JM, Delgado MA, Valencia C, Gallegos C. Thermal and mechanical characterization of cellulosic derivatives-based oleogels potentially applicable as bio-lubricating greases: Influence of ethyl cellulose molecular weight. *Carbohyd Polym* 2011; 83: 151–158.
- [35] Gallego R, Arteaga JF, Valencia C, Franco JM. Rheology and thermal degradation of isocyanate-functionalized methyl cellulose-based oleogels. *Carbohyd Polym* 2013; 98: 152–160.
- [36] Gallego R, González M, Arteaga JF, Valencia C, Franco JM. Influence of functionalization degree on the rheological properties of isocyanate-functionalized chitin- and chitosan-based chemical oleogels for lubricant applications. *Polymers* 2014; 6: 1929–1947.
- [37] Gallego R, Arteaga JF, Valencia C, Díaz MJ, Franco JM. Gel-like dispersions of HMDI-crosslinked lignocellulosic materials in castor oil: towards completely renewable lubricating grease formulations. *ACS Sustain Chem Eng* 2015; 3, 2130–2141.
- [38] Gallego R, Arteaga JF, Valencia C, Franco JM. Chemical modification of methyl cellulose with HMDI to modulate the thickening properties in castor oil. *Cellulose* 2013; 20: 495–507.
- [39] Howard GT. Biodegradation of polyurethane: a review. *Int. Biodeter. Biodegr.* 2002; 49: 245-252.
- [40] Ratajska, M, Boryniec, S. Physical and chemical aspects of biodegradation of natural polymers. *React. Funct. Polym.* 1998; 38:35-49.
- [41] Quinchia LA, Delgado MA, Valencia C, Franco JM, Gallegos C. Viscosity modification of different vegetable oils with EVA copolymer for lubricant applications. *Ind Crops Prod* 2010; 32: 607–612.

- 1  
2  
3  
4  
5  
6  
7  
8  
9  
10  
11  
12  
13  
14  
15  
16  
17  
18  
19  
20  
21  
22  
23  
24  
25  
26  
27  
28  
29  
30  
31  
32  
33  
34  
35  
36  
37  
38  
39  
40  
41  
42  
43  
44  
45  
46  
47  
48  
49  
50  
51  
52  
53  
54  
55  
56  
57  
58  
59  
60  
61  
62  
63  
64  
65
- [42] Gallego R, Arteaga JF, Valencia C, Franco JM. Thickening properties of several NCO-functionalized cellulose derivatives in castor oil. *Chem. Eng. Sci.* 2015; 134: 260–268.
- [43] Balan C, Franco JM. Influence of the geometry on the transient and steady flow of lubricating greases. *Tribol Trans* 2001; 44: 53–58.
- [44] Heyer P, Lauger J. Correlation between friction and flow of lubricating greases in a new tribometer device. *Lubr Sci* 2009; 21: 253–268.
- [45] Moreno G, Franco JM, Valencia C, Gallegos C. Rheology of lubricating greases modified with reactive NCO-terminated polymeric additives. *J Appl Polym Sci* 2010; 118: 693–704.
- [46] Chang GS, Koo JS, Song KW. Wall slip of vaseline in steady shear rheometry. *Korea-Aust Rheol J* 2003; 15: 55–61.
- [47] Goh SM, Versluis P, Appelqvist IAM, Bialek L. Tribological measurements of foods using a rheometer. *Food Res. Int.* 2010; 43: 183-186.
- [48] Maru, MM, Trommer, RM, Almeida, FA, Silva, RF, Achete, CA. ,Assessment of the lubricant behaviour of biodiesel fuels using Stribeck curves. *Fuel Process. Technol.* 2013; 116: 130-134.
- [49] Hutchings IM. *Tribology: Friction and wear of engineering materials*, Great Britain: Edward Arnold, 1992.
- [50] Sulek MW, Kulczycki A, Malysa A. Assessment of lubricity of compositions of fuel oil with biocomponents derived from rape-seed. *Wear* 2010; 268: 104–108.
- [51] Kalin M, Velkavrh I, Vizintin J. The Stribeck curve and lubrication design for non-fully wetted surfaces. *Wear* 2009; 267: 1232–1240.
- [52] Galda L, Pawlus P, Sep J. Dimples shape and distribution effect on characteristics of Stribeck curve. *Tribol Int* 2009; 42: 1505–1512.

1  
2 [53] García-Zapateiro LA, Franco JM, Valencia C, Delgado MA, Gallegos C. Viscous, thermal  
3 and tribological characterization of oleic and ricinoleic acids derived estolides and their blends  
4 with vegetable oils. J Ind Eng Chem 2013; 19: 1289–1298.  
5  
6

7 [54] Lu X, Khonsari, MM. An experimental investigation of grease-lubricated journal bearings.  
8  
9 J Tribol-T ASME 2007; 129: 84–90.  
10

11 [55] Gonçalves D, Graça B, Campos AV, Seabra J, Leckner J, Westbroek R. Formulation,  
12 rheology and thermal ageing of polymer greases - Part I: Influence of the thickener content.  
13 Tribol Int 2015; 87: 160–170.  
14  
15  
16  
17  
18  
19

20 [56] Palacios J, Palacios M. Rheological properties of greases in EHD contacts. Tribol Int 1984;  
21 17:167–71.  
22  
23  
24

25 [57] Gonçalves D, Graça B, Campos AV, Seabra J, Leckner J, Westbroek R. Formulation,  
26 rheology and thermal ageing of polymer greases - Part II: Influence of the co-thickener content.  
27 Tribol Int 2015; 87: 171–177.  
28  
29  
30  
31

32 [58] Quinchia LA, Delgado MA, Reddyhoff T, Gallegos C, Spikes HA. Tribological studies of  
33 potential vegetable oil-based lubricants containing environmentally friendly viscosity modifiers.  
34 Tribol Int 2014; 69: 110–117.  
35  
36  
37  
38  
39  
40  
41  
42  
43  
44  
45  
46  
47  
48  
49  
50  
51  
52  
53  
54  
55  
56  
57  
58  
59  
60  
61  
62  
63  
64  
65

1  
2  
3  
4  
5  
6  
7  
8  
9  
10  
11  
12  
13  
14  
15  
16  
17  
18  
19  
20  
21  
22  
23  
24  
25  
26  
27  
28  
29  
30  
31  
32  
33  
34  
35  
36  
37  
38  
39  
40  
41  
42  
43  
44  
45  
46  
47  
48  
49

**Table 1.** Formulation details of model biopolymer-based and commercial lubricating greases studied.

Substrate (g)	Thickener		Base oil	Formulation code	Penetration <sup>a</sup> (dmm)	Dropping point <sup>b</sup> (°C)
	Crosslinker (HMDI) (g)	Thickener concentration (% w/w)				
Methylcellulose (8.0)	4.1	30	castor oil	MC	271	185
Chitin (12.0)	7.6	30	castor oil	CH	219	223
Cellulosic pulp (5.0)	5.0	7	castor oil	CP	252	156
	Lithium soap	unkown	mineral oil	LI	260	195
	Calcium soap	unkown	castor oil	CA	324	145

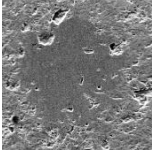
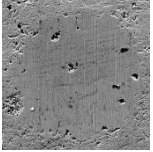
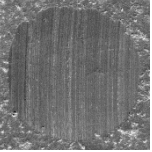
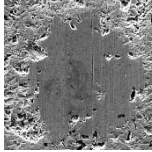
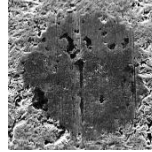
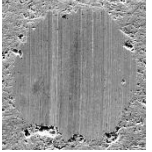
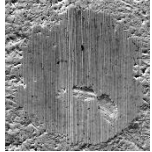
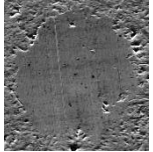
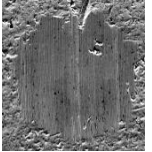
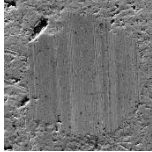
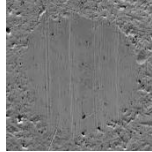
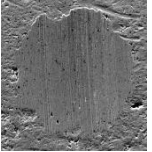
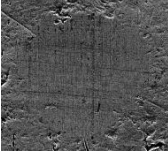
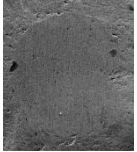
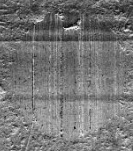
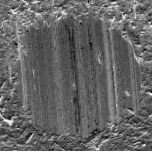
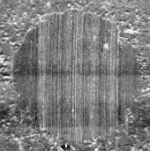

<sup>a</sup> According to ASTM D-217

<sup>b</sup> According to ASTM D-2265

**Table 2.** Power-law model fitting parameters of the viscous flow curves of biopolymer-based (CP, MC and CH) and commercial lubricating greases (LI and CA) studied at 25 and 125 °C.

<b>Sample</b>	<b>Temperature (°C)</b>	<b>n</b>	<b>K</b>	<b>R<sup>2</sup></b>
<b>LI</b>	25	0.067	704.0	0.9977
	125	0.248	98.1	0.9906
<b>CA</b>	25	0.137	720.0	0.9972
	125	0.131	35.4	0.9901
<b>CP</b>	25	0.107	782.4	0.9985
	125	0.130	26.3	0.9982
<b>MC</b>	25	0.066	960.9	0.9996
	125	0.125	52.7	0.9989
<b>CH</b>	25	0.079	2171.8	0.9972
	125	0.312	74.7	0.9958

**Table 3.** Selected SEM images and corresponding average diameter of wear scars on plates obtained at 25 and 125 °C, constant rotational speed (10 rpm) and different normal loads (10, 20 and 40 N) using samples CP, LI and CA as lubricants. Images are presented at different magnifications just to give an idea of the predominant wear mechanism.

25 °C			125 °C		
10 N	20 N	40 N	10 N	20 N	40 N
<b>CP</b>					
					
303 μm	331 μm	786 μm	254 μm	259 μm	410 μm
<b>LI</b>					
					
278 μm	273 μm	284 μm	285 μm	291 μm	343 μm
<b>CA</b>					
					
255 μm	321 μm	401 μm	304 μm	403 μm	716 μm

## FIGURE CAPTIONS

**Figure 1.** AFM micrographs for commercial lubricating greases: a) lithium grease; b) calcium grease. (Image width: 20  $\mu\text{m}$ ).

**Figure 2.** Viscous flow curves at 25 °C for commercial and model biopolymer-based lubricating greases studied.

**Figure 3.** Friction coefficient versus sliding velocity curves obtained for the different grease samples used as lubricants. (Normal force: 20 N; Temperature: 25 and 125 °C, respectively).

**Figure 4.** Stribeck curves for lubricating grease samples CA (**a**), MC (**b**) and CH (**c**).

**Figure 5.** Evolution of the friction coefficient with time, at 25 °C and a constant rotational speed (10 rpm) as a function of (**a**) lubricating greases (normal load: 10 N), and (**b**) normal force (sample MC).

**Figure 6.** Stationary friction coefficient values obtained by applying a constant rotational speed (10 rpm) and different normal loads (10, 20 and 40 N), at 25 and 125 °C, for the different lubricating greases studied.

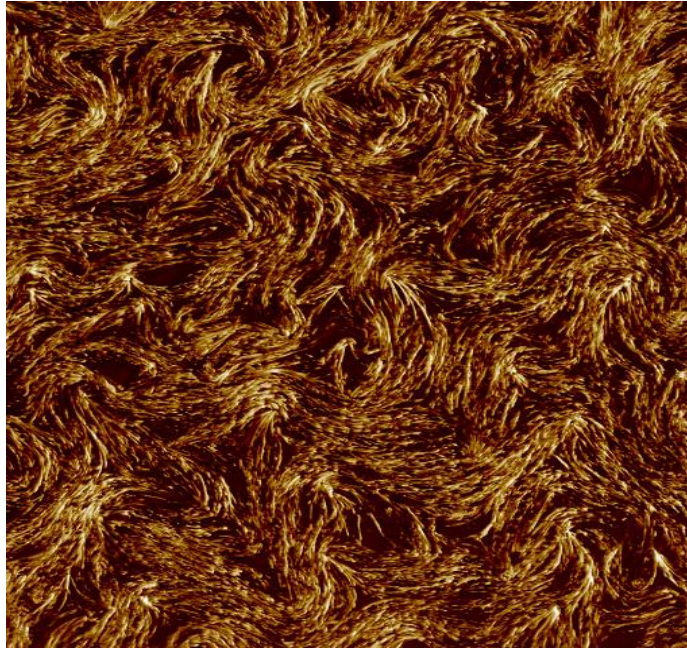
**Figure 7.** Stationary friction coefficient values obtained by applying 20 N constant normal force and different rotational speeds (0.15, 10 and 400 rpm), at 25 and 125 °C, for the different lubricating greases studied.

**Figure 8.** Average diameter of wear scars on plates obtained by applying a constant rotational speed (10 rpm) and different normal loads (10, 20 and 40 N), at 25 and 125 °C, for the different lubricating greases studied.

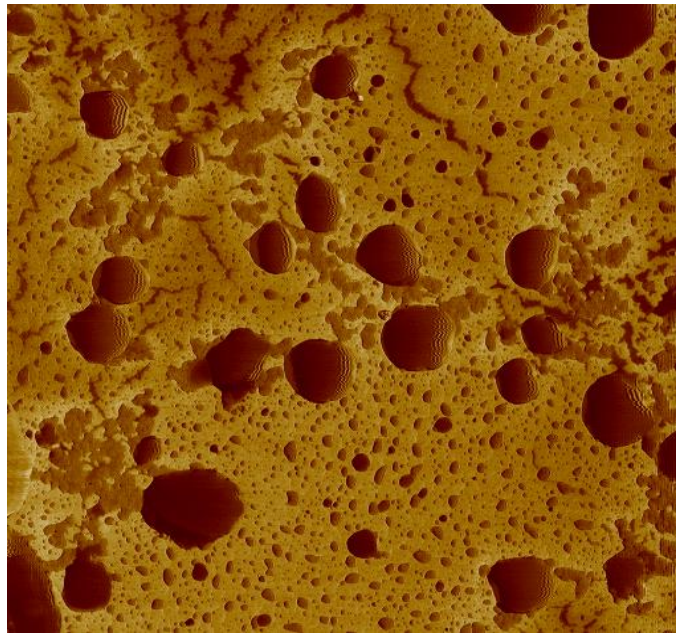
**Figure 9.** Average diameter of wear scars on plates obtained by applying 20 N constant normal force and different rotational speeds (0.15, 10 and 400 rpm), at 25 and 125 °C, for the different lubricating greases studied.



1  
2  
3  
4  
5  
6  
7  
8  
9  
10  
11  
12  
13  
14  
15  
16  
17  
18  
19  
20  
21  
22  
23  
24  
25  
26  
27  
28  
29  
30  
31  
32  
33  
34  
35  
36  
37  
38  
39  
40  
41  
42  
43  
44  
45  
46  
47  
48  
49  
50  
51  
52  
53  
54  
55  
56  
57  
58  
59  
60  
61  
62  
63  
64  
65



a)



b)

Figure 1

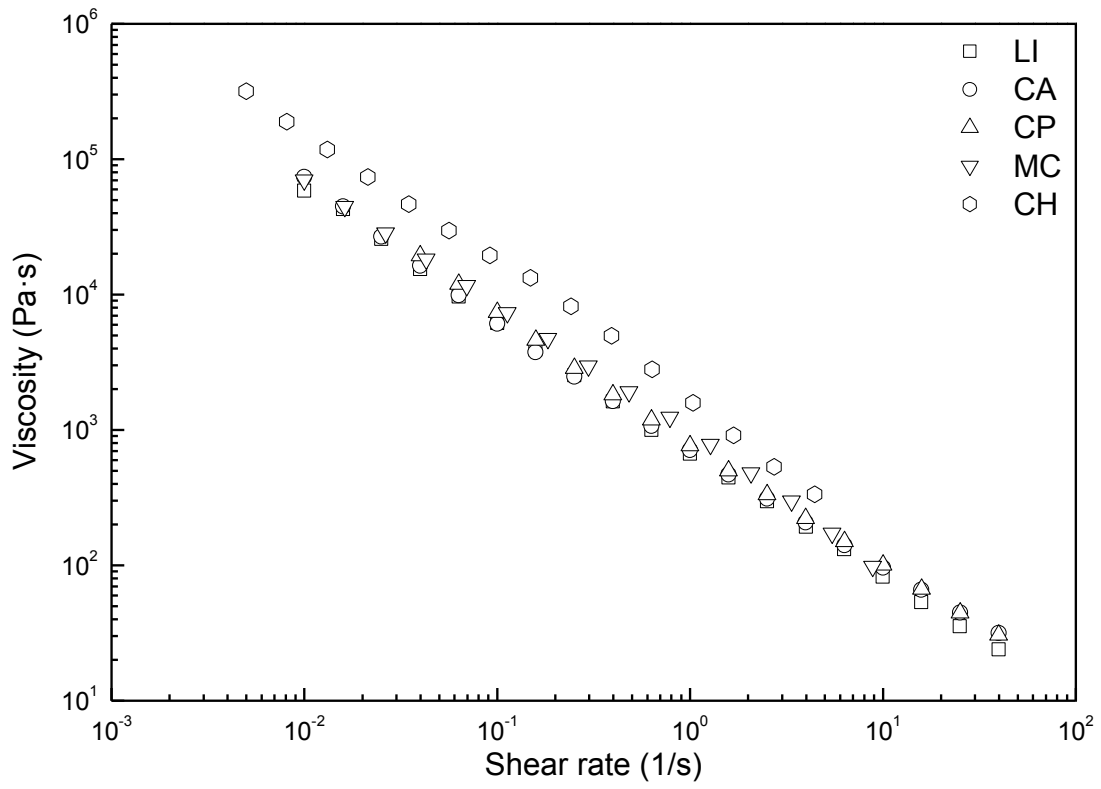


Figure 2

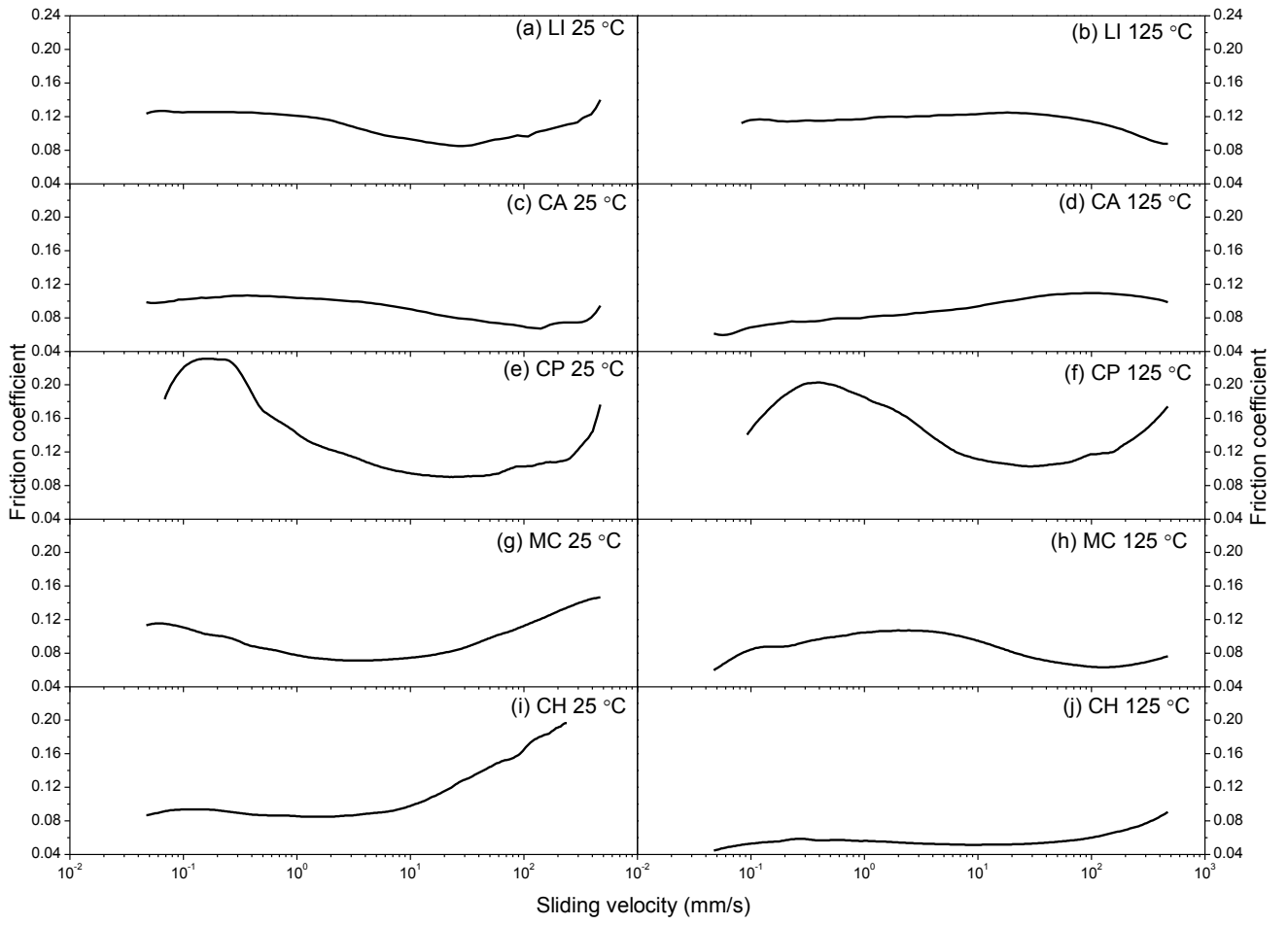


Figure 3

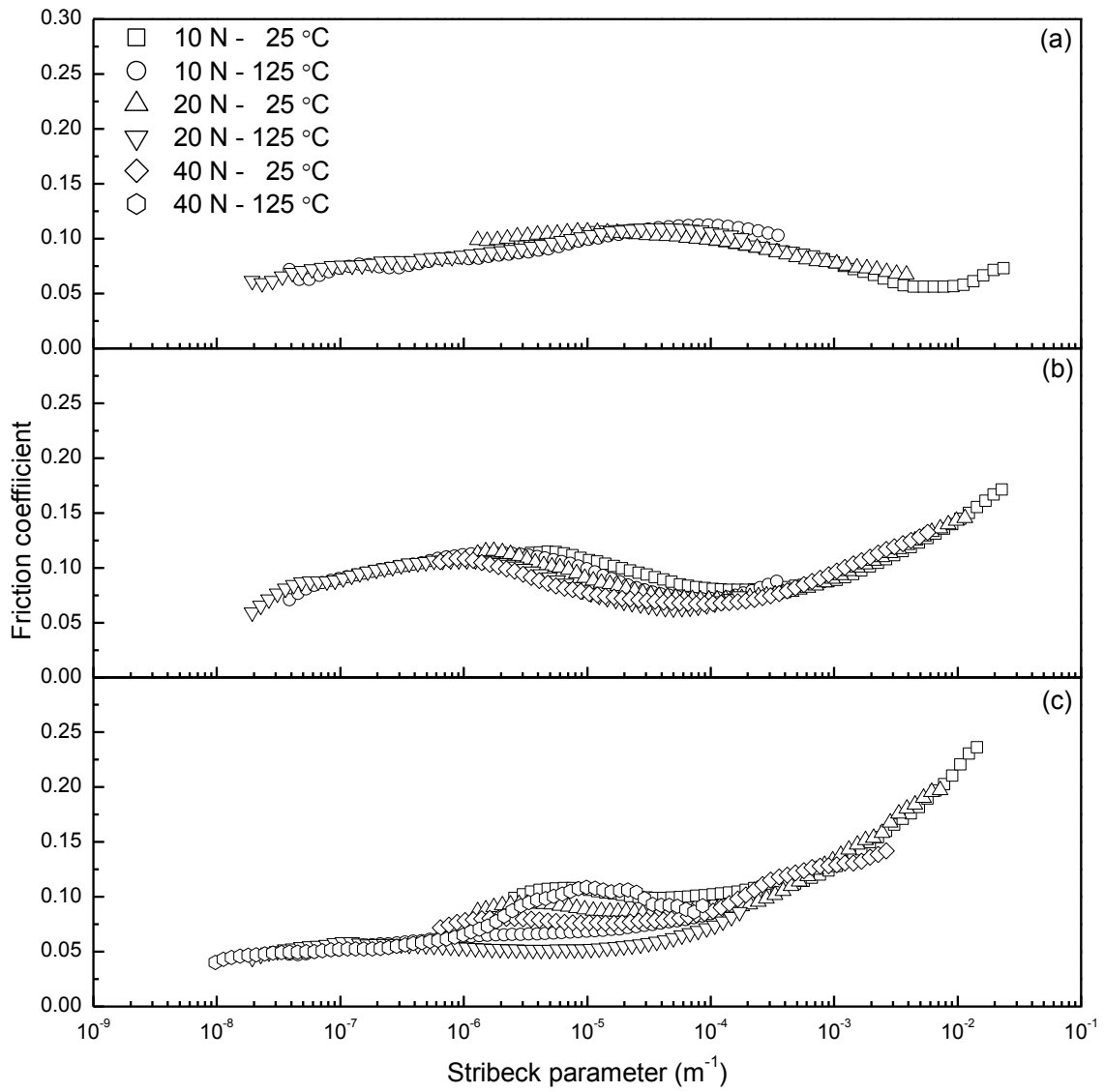


Figure 4

1  
2  
3  
4  
5  
6  
7  
8  
9  
10  
11  
12  
13  
14  
15  
16  
17  
18  
19  
20  
21  
22  
23  
24  
25  
26  
27  
28  
29  
30  
31  
32  
33  
34  
35  
36  
37  
38  
39  
40  
41  
42  
43  
44  
45  
46  
47  
48  
49  
50  
51  
52  
53  
54  
55  
56  
57  
58  
59  
60  
61  
62  
63  
64  
65

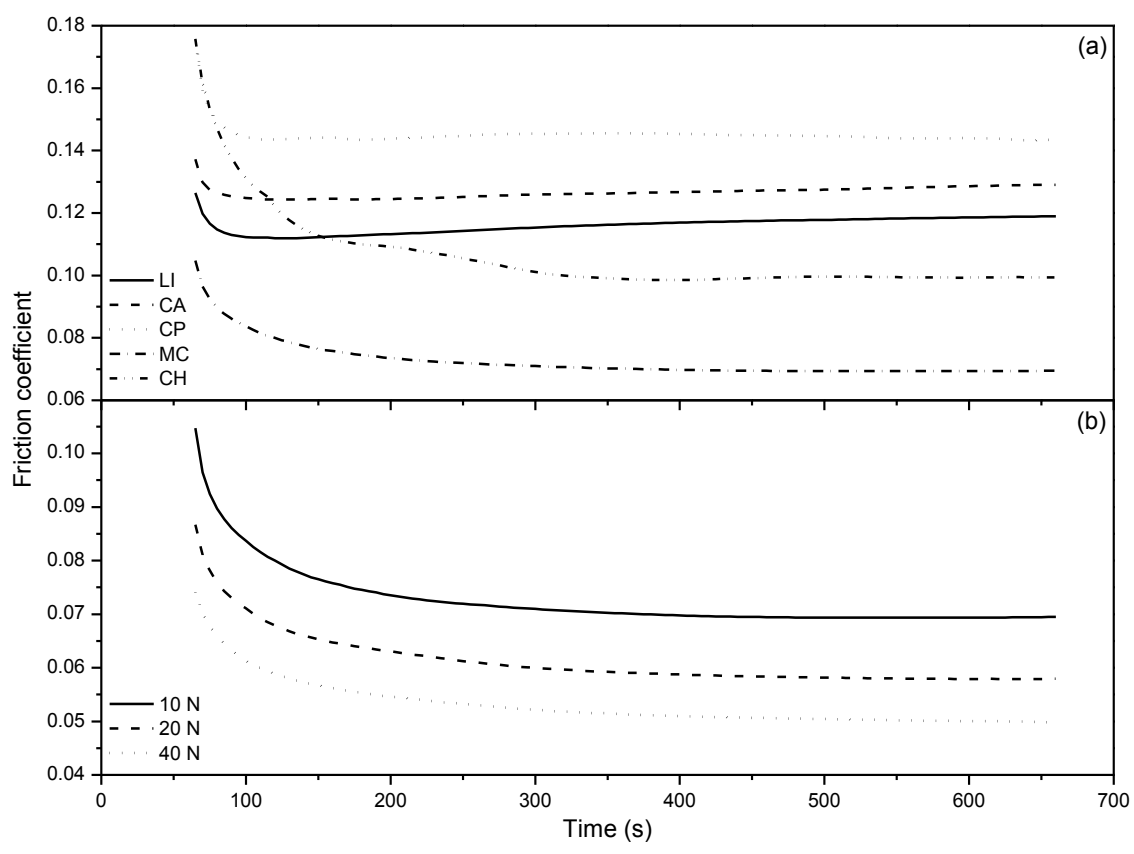


Figure 5

1  
2  
3  
4  
5  
6  
7  
8  
9  
10  
11  
12  
13  
14  
15  
16  
17  
18  
19  
20  
21  
22  
23  
24  
25  
26  
27  
28  
29  
30  
31  
32  
33  
34  
35  
36  
37  
38  
39  
40  
41  
42  
43  
44  
45  
46  
47  
48  
49  
50  
51  
52  
53  
54  
55  
56  
57  
58  
59  
60  
61  
62  
63  
64  
65

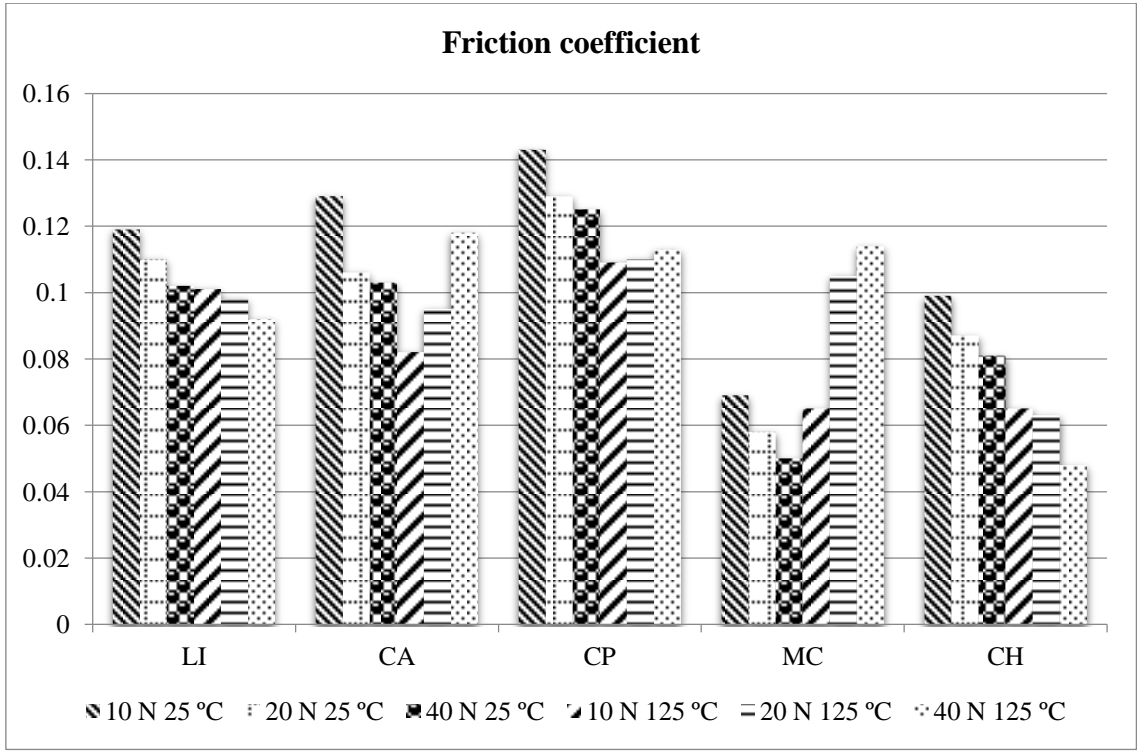


Figure 6

1  
2  
3  
4  
5  
6  
7  
8  
9  
10  
11  
12  
13  
14  
15  
16  
17  
18  
19  
20  
21  
22  
23  
24  
25  
26  
27  
28  
29  
30  
31  
32  
33  
34  
35  
36  
37  
38  
39  
40  
41  
42  
43  
44  
45  
46  
47  
48  
49  
50  
51  
52  
53  
54  
55  
56  
57  
58  
59  
60  
61  
62  
63  
64  
65

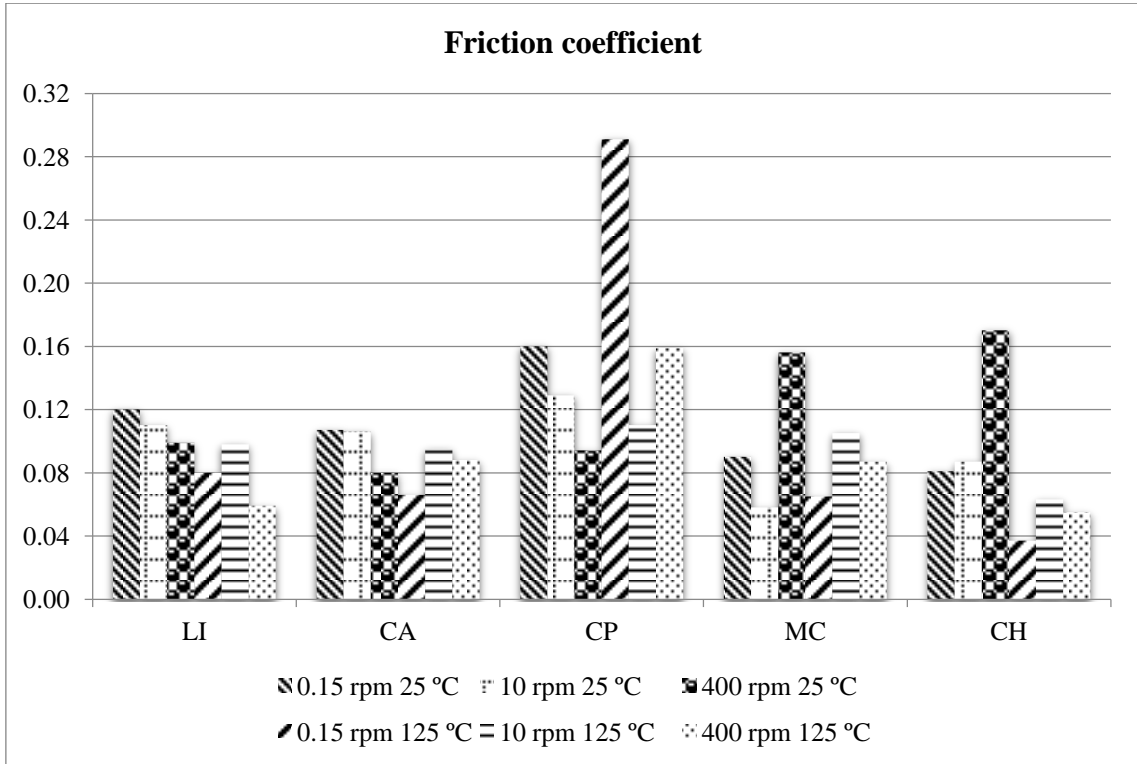


Figure 7

1  
2  
3  
4  
5  
6  
7  
8  
9  
10  
11  
12  
13  
14  
15  
16  
17  
18  
19  
20  
21  
22  
23  
24  
25  
26  
27  
28  
29  
30  
31  
32  
33  
34  
35  
36  
37  
38  
39  
40  
41  
42  
43  
44  
45  
46  
47  
48  
49  
50  
51  
52  
53  
54  
55  
56  
57  
58  
59  
60  
61  
62  
63  
64  
65

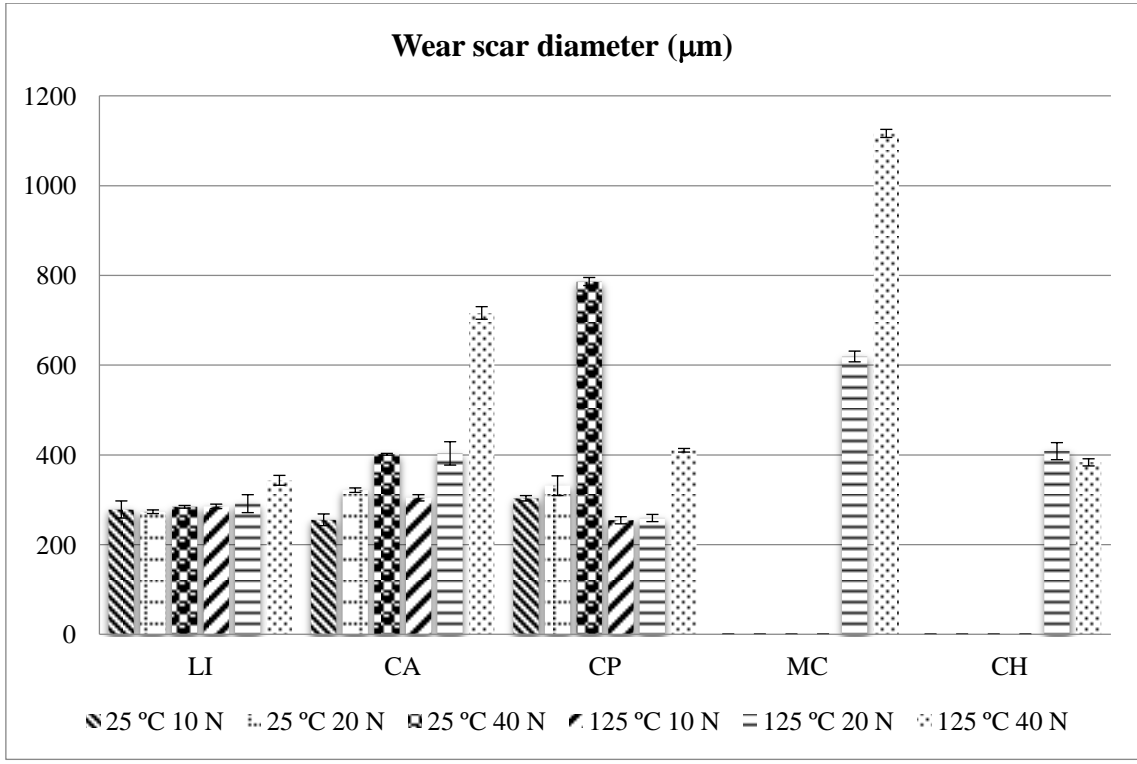


Figure 8



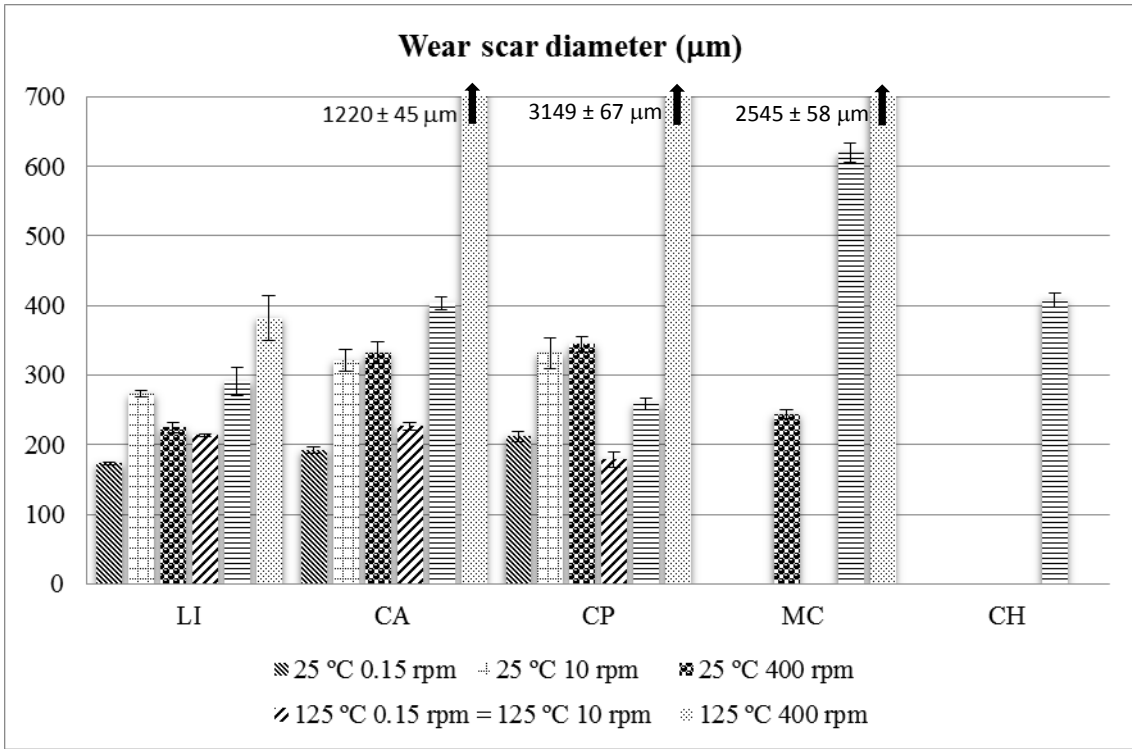


Figure 9